JOURNAL OF SOLID STATE CHEMISTRY 109, 307–314 (1994)

An X-Ray and Neutron Powder Diffraction Study of a New Polymorphic Phase of Copper Hydroxide Nitrate

N. Guillou, M. Louër, and D. Louër

Laboratoire de Cristallochimie (U.R.A. C.N.R.S. 1495), Université de Rennes I, Avenue du Général Leclerc, 35042 Rennes Cédex, France

Received May 6, 1993; in revised form July 28, 1993; accepted July 29, 1993

High-temperature sequential powder diffractometry has revealed a phase transformation in monoclinic copper hydroxide nitrate $Cu_2(OH)_3(NO_3)$ occurring at 158°C. It is connected with a small endothermic effect of 0.5 KJ mole^{-1}. The high-temperature phase is monoclinic with the unit cell dimensions a = 5.6132(7), b = 6.0986(8), c = 6.9560(9) Å, and β = 92.35(1)°; the space group is $P2_1$ with Z = 2. The crystal structure of this new phase has been determined from X-ray and neutron powder diffraction data collected at 160°C. The structure is built from wavy layers of brucite type, linked together by hydrogen bonds, as in the room-temperature phase. The main differences between the two phases are a slight reorientation of the nitrate group and some changes occurring in hydrogen bonds. © 1994 Academic Press, Inc.

INTRODUCTION

Two varieties of copper (II) hydroxide nitrate $Cu_2(OH)_3(NO_3)$ are known: the orthorhombic mineral gerhardite and the synthetic monoclinic phases. Thermal analyses of the monoclinic form, by means of thermogravimetry and differential scanning calorimetry, have been reported by several authors (1–3). Only the effect of the decomposition reaction was observed and carefully interpreted. This reaction in vacuum takes place in the range 170–190°C and gives copper oxide through a mechanism involving the formation, inside the crystals, of nitric acid and water molecules with a heat of reaction ΔH = 172.4 KJ mole^{-1} (2). The oxide obtained from this thermal decomposition was at the origin of the detection of anomalous X-ray diffraction line shapes in annealed copper (II) oxide reported recently (4). The structure of the monoclinic phase was solved first by Nowacki and Scheidegger (5) in the space group $P2_1/m$, and revised by Effenberger (6) in the noncentrosymmetric space group $P2_1$. An order–disorder phase transformation was identified at a low temperature (150 K) (7). The structure of the orthorhombic phase was studied by Bovio and Locchi (8), in the space group $P2_12_12_1$. The structure of the two phases consists of layers with composition $[Cu_2(OH)_3O]$ linked together by hydrogen bonds through NO_3 ions. The main difference between the two phases is a shift of one layer out of two in the orthorhombic phase; this causes the b axis to be doubled. The present study deals with a reinvestigation of the thermal behavior of the monoclinic variety of means of high-temperature sequential thermodiffractometry. The power of this technique to elucidate reaction mechanisms has been demonstrated in various studies (see, for example, Refs. 9 and 10). A new polymorphic phase of copper hydroxide nitrate has been identified and its structure has been studied by means of conventional X-ray powder diffraction and neutron powder diffraction data collected at the Laboratoire Léon Brillouin.[1]

EXPERIMENTAL

Copper hydroxide nitrate $Cu_2(OH)_3NO_3$ was prepared by reaction, at 170°C, of a concentrated aqueous solution of copper nitrate with cupric oxide. A green polycrystalline solid was obtained after a few days and identified as the monoclinic phase by X-ray powder diffraction, although a small proportion of the orthorhombic phase could also be detected. For the neutron diffraction study, deuterated copper hydroxide nitrate was prepared using D_2O instead of H_2O.

High-temperature sequential power diffractometry was carried out by means of a INEL (CPS120) curved position-sensitive detector, which allows for simultaneous recording of powder diffraction pattern over a range of 120°. The detector was used in a semifocusing arrangement by reflection, described elsewhere (9). The X-ray generator operated at 40 kV and 36 mA, and a monochromatic Cu$K\alpha_1$ radiation (λ = 1.54059 Å) was selected with an incident beam curved-crystal quartz monochromator with asymmetric focusing (short focal distance = 130 mm, long focal distance = 510 mm). A fixed angle of 7° was selected between the incident beam and the surface of the stationary sample. The sample was located in a monitored high-temperature X-ray diffractometer attachment (Rigaku)

[1] Laboratoire commun CEA-CNRS.

0022-4596/94 $6.00

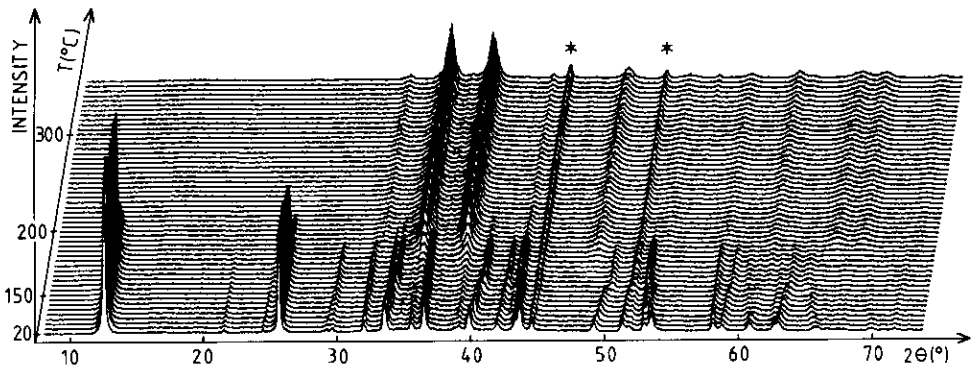

FIG. 1. 3D plot of the powder diffraction patterns vs temperature for monoclinic copper hydroxide nitrate $Cu_2(OH)_3(NO_3)$ in a vacuum (heating rate = 100°C hr^{-1} between room temperature and 150°C, 10°C hr^{-1} in the range 150–200°C, and 15°C hr^{-1} at higher temperatures; counting time for each pattern = 1000 sec). *Spurious diffraction lines from sample holder.

designed to maintain the specimen in a vacuum, inert gas, or ambient atmosphere (10). The experiment was carried out in a vacuum with heating rates of 100°C hr^{-1} between room temperature and 150°C, 10°C hr^{-1} in the range 150–200°C, and 15°C hr^{-1} at higher temperatures. Time for data acquisition for each pattern was 1000 sec. Data were stored in a DEC PDP 11-73 computer, and the 3D plot of collected data was performed by means of a program written locally for a HP 7475A plotter. For structure analyses, precise X-ray powder diffraction data were collected at room temperature with a Siemens D500 powder diffractometer ($CuK\alpha_1$ radiation) described elsewhere (11) and at 160°C, in air, on a CGR (Compagnie Générale de Radiologie) instrument ($CuK\alpha_1$ radiation) equipped with a high-temperature attachment (12). Powder neutron diffraction data were collected in argon atmosphere, at the same temperatures, with the High Resolution Powder Diffractometer 3T2 (λ = 1.2266 Å) of the Laboratoire Léon Brillouin. Differential scanning calorimetry was performed with a Perkin–Elmer DSC7 instrument at a heating rate of 10°C min^{-1} in a sealed container.

HIGH TEMPERATURE X-RAY POWDER DIFFRACTION

The three-dimensional representation of the powder diffraction patterns with temperature (Fig. 1) shows that a sudden shift of several reflections of the monoclinic phase occurs at about 158°C, mainly for the lines with h and $l \neq 0$, without significant changes in diffraction line intensities. This phase transformation is reversible and is connected with an endothermic energy effect of 0.5 KJ $mole^{-1}$ and an onset temperature of 158.3°C (Fig. 2). This value is very weak compared with the decomposition heat given above. It explains why this effect was not observed in previous studies (1–3).

The X-ray diffraction powder pattern of the high-temperature phase (HT) obtained in air at 160°C was indexed by the computer program DICVOL91 (13). The first twenty lines were used with an absolute error on observed lines of 0.03° (2θ), after low angle correction for axial divergence effect, from 00l orders identified in the pattern. A monoclinic cell was obtained with satisfactory figures of merit [M_{20} = 31, F_{20} = 26(0.0132, 58)]. The complete dataset was reviewed by means of the computer program NBS*AIDS83 (14). From this evaluation and refinement the cell dimensions are a = 5.6132(7), b = 6.0986(8), c = 6.9560(9) Å, β = 92.35(1)°, V = 237.92(4) Å^3 with M_{20} = 37 and F_{30} = 25 (0.0140, 85). The list of calculated and observed peak positions is given in Table 1. Because the reported powder data of the room-temperature phase (RT) (PDF 15-14) are of low precision [F_{30} = 23(0.025, 52)], new X-ray powder diffraction data were collected and reviewed, giving the final cell parameters a = 5.5985(7), b = 6.0804(7), c = 6.9312(8)Å, β = 94.64(1)°, and V = 235.17(4) Å^3 (M_{20} = 72 and F_{30} = 71 (0.0082,52)). The powder diffraction data are given in Table 2. The lower

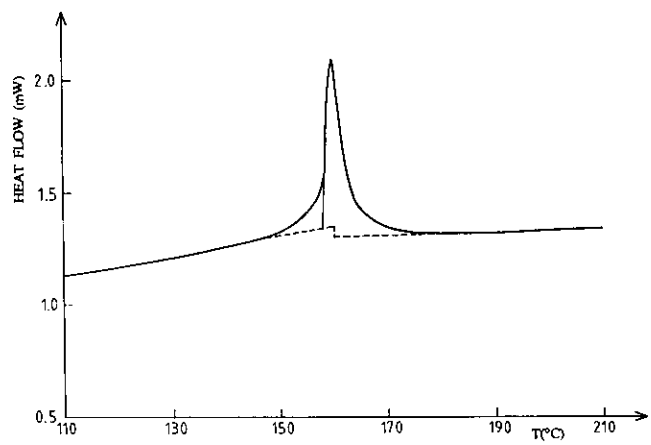

FIG. 2. DSC curve obtained at the heating rate of 10°C min^{-1} for the monoclinic form of $Cu_2(OH)_3(NO_3)$.

TABLE 1
X-Ray Powder Diffraction Pattern of $Cu_2(OH)_3(NO_3)$ at 160°C

hkl	$2\theta_{obs}$(°)	$2\theta_{calc}$(°)	d_{obs}(Å)	I_{obs}
001	12.728	12.727	6.95	100
100	15.765	15.789	5.62	1L
011	19.298	19.348	4.596	1L
101	20.707	20.739	4.286	1L
$\bar{1}10$	21.480	21.508	4.134	2
$\bar{1}11$	24.691	24.729	3.603	1
002	25.614	25.614	3.475	37
020	29.276	29.264	3.048	1L
012	29.565	29.562	3.019	2
102	30.789	30.795	2.902	1L
200	31.886	31.888	2.804	4
120	33.433	33.421	2.678	6
$\bar{2}01$	33.953	33.951	2.638	7
201	34.963	34.963	2.564	1
$\bar{1}21$	35.641	35.652	2.517	1
121	36.134	36.140	2.4838	12
003	38.850	38.841	2.3162	2
$\bar{2}02$	40.456	40.464	2.2279	6
$\bar{1}22$	42.129	42.152	2.1432	6
122	42.988	42.998	2.1023	8
$\bar{3}01$	49.948	49.956	1.8245	2
310	51.034	51.058	1.7882	1L
$\bar{1}23$	51.580	51.608	1.7705	2
222	52.163	52.179	1.7521	1
004	52.637	52.633	1.7374	5
$\bar{3}20$	57.795	57.804	1.5940	3
$\bar{3}21$	58.936	58.953	1.5658	2
321	59.929	59.950	1.5423	1
040	60.686	60.693	1.5248	1
$\bar{2}04$	61.585	61.576	1.5047	1
041	62.294	62.295	1.4893	2
$\bar{1}24$	63.171	63.156	1.4707	2
204	64.155	64.150	1.4505	1
124	64.446	64.433	1.4446	1
322	65.202	65.194	1.4297	1
400	66.664	66.650	1.4018	1L
042	66.987	66.970	1.3959	1
005	67.327	67.306	1.3896	1
$\bar{4}01$	67.564	67.556	1.3853	1L
401	68.820	68.790	1.3631	1L
015	69.271	69.274	1.3553	1L
240	70.225	70.210	1.3392	1L
$\bar{3}23$	70.484	70.476	1.3349	1L
$\bar{2}41$	71.420	71.397	1.3197	1

TABLE 2
X-Ray Powder Diffraction Pattern of $Cu_2(OH)_3(NO_3)$ at Room Temperature

hkl	$2\theta_{obs}$(°)	$2\theta_{calc}$(°)	d_{obs}(Å)	I_{obs}
001	12.810	12.804	6.91	100
011	19.426	19.432	4.566	1L
101	21.259	21.245	4.176	1L
110	21.596	21.598	4.112	2
$\bar{1}11$	24.512	24.507	3.629	1
002	25.774	25.771	3.454	47
$\bar{1}02$	29.259	29.262	3.050	1
020	29.352	29.354	3.040	1L
012	29.723	29.722	3.003	2
102	31.519	31.520	2.836	1L
200	32.052	32.054	2.790	3
021	32.160	32.141	2.781	1L
$\bar{1}20$	33.549	33.541	2.669	7
$\bar{2}01$	33.631	33.628	2.663	5
210	35.363	35.368	2.536	1L
$\bar{1}21$	35.558	35.550	2.523	2
201	35.650	35.638	2.516	1
121	36.523	36.521	2.4582	11
$\bar{2}11$	36.824	36.817	2.4388	1L
211	38.710	38.683	2.3242	1
003	39.089	39.085	2.3026	2
$\bar{2}02$	39.817	39.823	2.2621	6
013		41.917		
$\bar{1}22$	41.923	41.927	2.1532	3
202	43.265	43.268	2.0895	2
122	43.609	43.609	2.0738	8
$\bar{2}21$	45.211	45.230	2.0040	1L
212	45.895	45.889	1.9757	1L
113	46.256	46.287	1.9611	1L
$\bar{2}03$	49.150	49.181	1.8522	4
$\bar{3}10$	51.330	51.326	1.7785	3
$\bar{1}23$		51.343		
004	52.973	52.975	1.7272	4
123	53.509	53.505	1.7111	5
104	57.039	57.036	1.6133	1L
$\bar{2}31$		57.060		
$\bar{3}20$	58.080	58.090	1.5869	4
$\bar{2}23$	58.359	58.313	1.5799	1L
231		58.411		
$\bar{3}21$	58.745	58.756	1.5705	3
$\bar{2}04$	60.706	60.686	1.5244	2
040	60.895	60.895	1.5201	2
041	62.504	62.513	1.4848	2
$\bar{3}22$	62.658	62.675	1.4815	1
$\bar{1}24$	62.884	62.897	1.4767	3

accuracy of the HT powder data ($<\Delta(2\theta)> = 0.0140°$) compared to those obtained for the RT phase ($<\Delta(2\theta)> = 0.0082°$) is explained by the less favorable experimental conditions. For the HT phase, *a*, *b*, and *c* parameters are slightly elongated by 0.26, 0.30, and 0.36%, respectively, and a more significant change is observed for the β angle, which decreases from 94.64 to 92.35°. Although this is the consequence of a small change in the crystal structure in the RT phase, a complete *ab initio* structure determination of the HT phase was undertaken.

STRUCTURE INVESTIGATION

The crystal structure determination of the HT phase has been carried out from the X-ray powder diffraction data. Integrated intensity data were extracted by means of an iterative pattern decomposition procedure implemented in the Rietveld program FULLPROF (15), which is a derived version of the DBW3.2S(8804) program (16).

A list of 181 values of F_{obs} was obtained and used for solving the structure. The use of direct methods allowed for the location of the two independent copper atoms and their environment, which form $[Cu_2(OH)_3O]$ layers of brucite type. The refinement, carried out with these initial positions, converged to a crystal-structure model indicator $R_F = 0.2$. Fourier syntheses alternating with cycles of refinement allowed for the location of the nitrogen atom but gave no significant peaks for the two terminal oxygens of the nitrate group. Consequently, neutron diffraction data were used to locate the two terminal oxygen atoms and to refine the final structure model. The first stage of the study was performed with the WYRIET software (17), used on a PC computer, allowing Rietveld refinement and Fourier synthesis using neutron diffraction data. The two independent copper atoms and their environment, previously found from the X-ray diffraction analysis, and the deuterium atoms at the positions estimated from Effenberger's results (6), were used for the first refinement, which converged to the structure model factor $R_F = 0.38$. A Fourier synthesis gave a significant peak corresponding to the position of the nitrogen atom. This caused R_F to decrease to 0.20. A new Fourier synthesis gave two diffuse peaks, close to the positions of the two terminal oxygen atoms of the nitrate group in the RT phase. These initial positions were refined with the program FULLPROF. A pseudo-Voigt function was selected to fit individual line profiles. In order to describe the angular dependence of the peak full-width at half-maximum, the usual quadratic form in tan θ was used with initial values of the constants, U, V, and W derived from Bragg components obtained by pattern decomposition. Unit cell and instrument parameters were allowed to vary from time to time during the refinement process. The final Rietveld refinement involved the following parameters: 35 atomic coordinates, 6 isotropic temperature factors, 1 scale factor, 1 zero point parameter, 4 cell parameters, 3 half-width and 1 asymmetry parameters, 6 coefficients used to define the functional dependence of the background, the line-shape factor η, and the preferred-orientation parameter. For comparison, the refinement of the RT phase from the neutron diffraction data was also carried out, starting with Effenberger's model. From this study it was found that the substitution of H by D atoms was not complete. The refined occupation parameter implied a value of 0.767 for the deuterium atom. This value was then used for the study of the HT phase. In the final stage of the refinement of the RT phase, the scale factor of the orthorhombic phase was also refined. Its magnitude, 0.0007, compared with the value 0.0951 found for the monoclinic phase, gives an indication about the amount of the additional phase. The details of the final refinements are given in Table 3. Figures 3 and 4 show the final fit obtained between calculated and observed patterns, respectively, for the RT and HT phases. These fits correspond to satisfactory crystal-structure model indicators ($R_F = 0.044$, $R_B = 0.057$) and ($R_F = 0.063$, $R_B = 0.078$), and profile factors ($R_P = 0.021$, $R_{WP} = 0.028$) and ($R_P = 0.023$ and $R_{WP} = 0.029$), respectively, for the RT and HT phases. Final atomic parameters of the two phases are given in Table 4, where they are compared to the results obtained for the RT phase by Effenberger (6). Table 5 gives selected bonds and angles determined by neutron diffraction for the two phases.

TABLE 3
Details of Rietveld Full-Profile Refinement for the Two Phases from Neutron Diffraction Data

	RT phase	HT phase
a (Å)	5.6005(2)	5.6137(3)
b (Å)	6.0797(2)	6.0982(3)
c (Å)	6.9317(3)	6.9575(4)
β (°)	94.619(3)	92.375(4)
Space group	$P2_1$	$P2_1$
Z	2	2
Wavelength (Å)	1.2266	1.2266
2θ range (°)	8–125	8–110
Step scan increment (°2θ)	0.05	0.05
No. of reflections	866	698
No. of structural parameters	42	42
No. of atoms	12	12
R_F	0.044	0.063
R_B	0.057	0.078
R_P	0.021	0.023
R_{WP}	0.028	0.029

DISCUSSION

The structural analysis carried out at room and high temperatures shows that small structural changes occur in monoclinic copper hydroxide nitrate at 158°C. It can be noted that the atomic positions obtained from neutron powder diffraction for the RT phase are generally in agreement with Effenberger's results within 3σ (see Table 4), although the results from neutron powder diffraction data are less precise for copper atom positions. Consequently, the structural differences observed between the RT and HT phases may be regarded as significant. As for the RT phase, the structure of the HT phase consists of slightly wavy layers of copper atoms approximately in the (001) plane, linked together by hydrogen bonds through the nitrate groups. Each copper atom is octahedrally coordinated: Cu(1) atoms are surrounded by four OH^- and two oxygen atoms of the NO_3^- groups; Cu(2) atoms are coordinated by four OH^-, a fifth OH^- at a greater distance, and one oxygen atom of the NO_3^-. For the $Cu(1)O_6$ polyhedron, four equatorial distances range

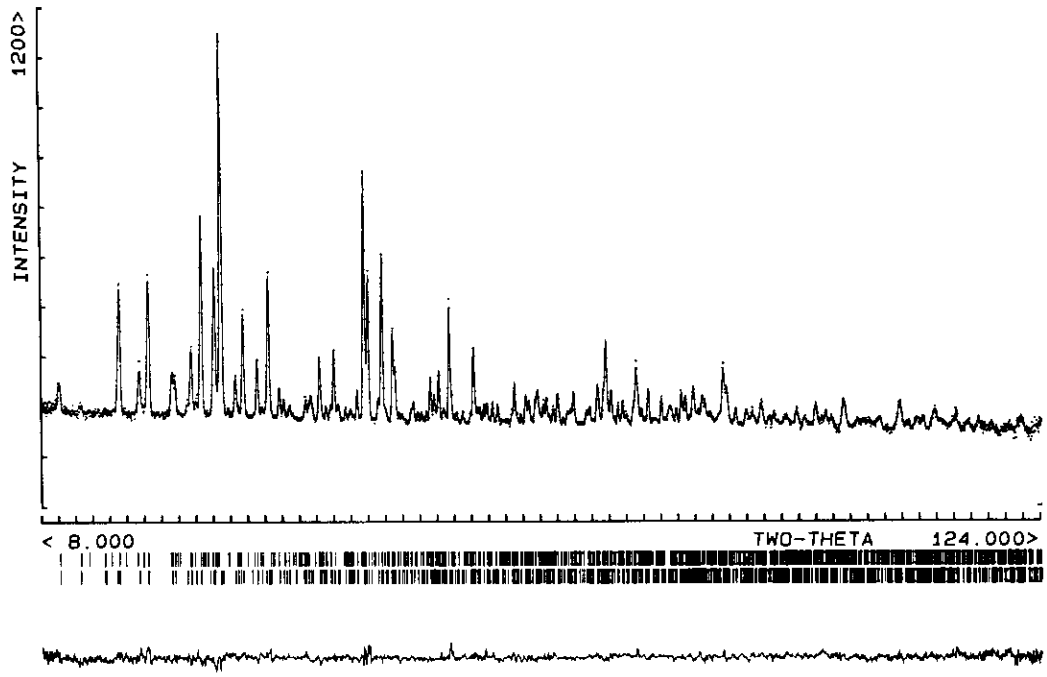

FIG. 3. The final Rietveld difference plot for the room-temperature phase of copper hydroxide nitrate. In the upper portion, the observed data are shown by the dots; the calculated pattern is displayed by the solid line; the lower curve is a plot of the difference, observed minus calculated. The vertical markers below the profile indicate the positions calculated for Bragg reflections, for the monoclinic phase (bottom), and for the spurious orthorhombic phase.

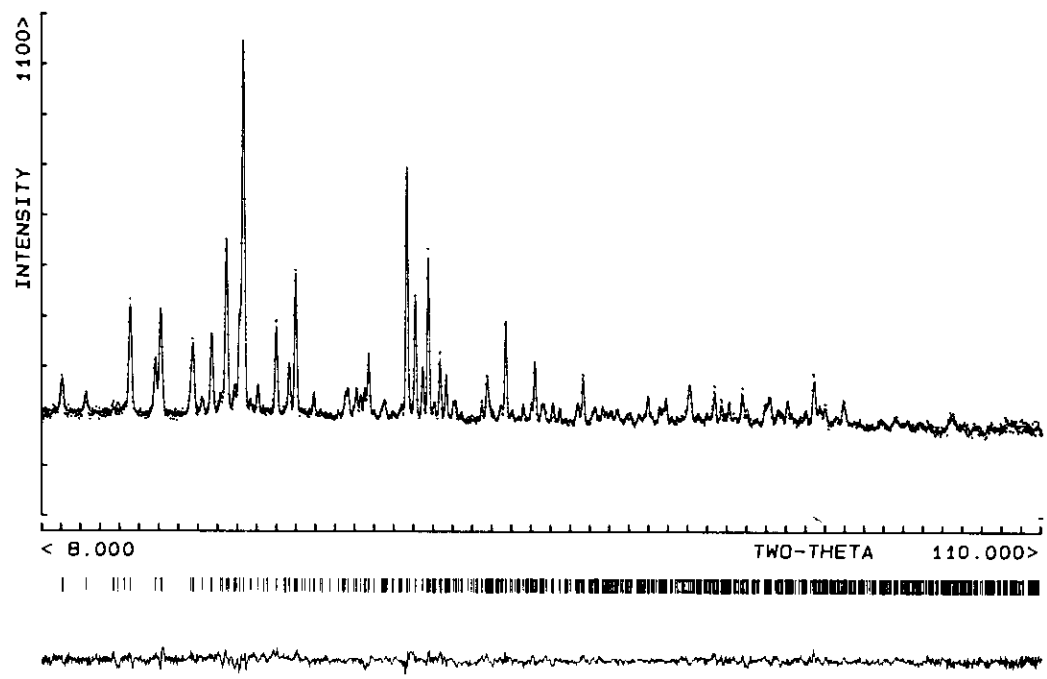

FIG. 4. The final Rietveld difference plot for the high-temperature phase of copper hydroxide nitrate.

TABLE 4

Final Atomic Parameters Obtained by Powder Neutron Diffraction for the Room-Temperature (NRT) and High-Temperature (NHT) Phases Compared with the Results Obtained by Effenberger (6) from Single Crystal X-Ray Diffraction Data (RX).

Atom		x	y	z	B_{iso}(Å^2)
	RX	−0.0015(3)	0.0000	0.9945(2)	0.87
Cu(1)	NRT	−0.003(2)	0.0000	0.989(1)	0.69(4)[a]
	NHT	−0.001(2)	0.0000	0.975(1)	1.02(7)[a]
	RX	0.5091(1)	0.2483(4)	−0.0024(2)	0.83
Cu(2)	NRT	0.5086(7)	0.248(3)	−0.0027(8)	0.69(4)[a]
	NHT	0.509(1)	0.253(3)	−0.005(1)	1.02(7)[a]
	RX	0.869(1)	0.252(2)	0.857(1)	1.06
OH(1)	NRT	0.8684(9)	0.260(3)	0.8567(9)	0.80(5)[b]
	NHT	0.873(1)	0.254(3)	0.859(1)	1.31(8)[b]
	RX	0.313(1)	0.013(2)	0.879(1)	0.83
OH(21)	NRT	0.306(2)	0.002(3)	0.879(2)	0.80(5)[b]
	NHT	0.316(3)	−0.002(3)	0.880(2)	1.31(8)[b]
	RX	−0.313(1)	0.002(2)	−0.881(1)	0.89
OH(22)	NRT	−0.318(2)	−0.002(3)	−0.876(2)	0.80(5)[b]
	NHT	−0.324(3)	−0.005(3)	−0.878(2)	1.31(8)[b]
H(1)	RX	0.89(2)	0.29(4)	0.76(2)	1.00
D(1)	NRT	0.900(2)	0.259(4)	0.724(2)	2.7(1)[c]
	NHT	0.912(3)	0.231(5)	0.724(3)	4.5(3)[c]
H(21)	RX	0.31(2)	0.03(4)	0.78(2)	1.00
D(21)	NRT	0.293(3)	0.024(4)	0.738(3)	2.7(1)[c]
	NHT	0.290(4)	0.016(5)	0.744(4)	4.5(3)[c]
H(22)	RX	−0.28(2)	0.01(4)	−0.77(2)	1.00
D(22)	NRT	−0.290(3)	−0.008(4)	−0.739(3)	2.7(1)[c]
	NHT	−0.323(4)	0.005(6)	−0.748(5)	4.5(3)[c]
	RX	0.231(1)	0.259(3)	0.408(1)	2.00
N	NRT	0.2330(7)	0.261(2)	0.4069(7)	2.18(8)
	NHT	0.207(1)	0.264(4)	0.404(1)	4.8(2)
	RX	0.207(1)	0.251(2)	0.223(1)	1.40
O(1)	NRT	0.204(1)	0.248(3)	0.225(1)	1.2(1)
	NHT	0.198(2)	0.245(4)	0.229(2)	2.3(2)
	RX	0.387(1)	0.157(2)	0.496(1)	4.01
O(21)	NRT	0.391(2)	0.156(2)	0.494(2)	3.2(1)[d]
	NHT	0.372(3)	0.198(3)	0.498(3)	7.2(3)[d]
	RX	−0.097(2)	−0.112(2)	−0.492(1)	3.78
O(22)	NRT	−0.096(2)	−0.122(2)	−0.491(2)	3.2(1)[d]
	NHT	−0.027(3)	−0.156(3)	−0.478(3)	7.2(3)[d]

[a,b,c,d] Some thermal parameters are allowed to vary in the same manner.

from 1.87(2) to 2.11(2) Å (mean value : 1.98 Å) and apical distances are equivalent to 2.54(2) and 2.35(2) Å. For the $Cu(2)O_6$ polyhedron, the dispersion of distances is lower. Indeed, four equatorial distances range from 1.96(2) to 2.04(2) Å (mean value : 2.00 Å) and axial distances are equivalent to 2.44(1) and 2.29(1) Å. It can be noted that these results are in good agreement with the statistical results recently reported by Eby and Hawthorne (18). In this study a hierarchical structural classification for copper oxysalt minerals is described, from which it is observed that, in an octahedral environment, there is a very strong bimodal distribution of Cu–O distances with maxima at 1.97 and 2.44 Å (see Fig. 34 in Ref. 18), which corresponds to a [4 + 2]-coordination. In the structure of the HT phase, the $Cu(1)O_6$ polyhedron seems to be more affected by the phase transformation, as shown by the higher dispersion of equatorial and axial distances, than those found in the RT phase. On the contrary, $Cu(2)O_6$

TABLE 5
Selected Bond Distances (Å) and Angles (°) with Their Standard Deviations for the RT and HT Phases

	RT	HT		RT	HT
			Within the CuO_6 polyhedra		
Cu(1)–OH(1)	1.94(2)	1.87(2)	Cu(2)–OH(21)	2.01(2)	2.04(2)
Cu(1)–OH(1)	1.92(2)	2.01(2)	Cu(2)–OH(21)	2.01(2)	1.97(2)
Cu(1)–OH(21)	1.94(1)	1.93(2)	Cu(2)–OH(22)	1.97(2)	2.02(2)
Cu(1)–OH(22)	2.06(1)	2.11(2)	Cu(2)–OH(22)	2.00(2)	1.96(2)
Cu(1)–O(1)	2.45(2)	2.54(2)	Cu(2)–O(1)	2.413(8)	2.44(1)
Cu(1)–O(1)	2.36(2)	2.35(2)	Cu(2)–OH(1)	2.309(7)	2.29(1)
			Within the NO_3 group		
N–O(1)	1.262(9)	1.22(2)	O(1)–N–O(21)	119(1)	122(2)
N–O(21)	1.22(2)	1.18(2)	O(1)–N–O(22)	119(1)	116(2)
N–O(22)	1.21(1)	1.26(2)	O(21)–N–O(22)	121.8(9)	122(2)
			Within the hydroxyl groups		
D(1)–OH(1)	0.95(1)	0.98(2)			
D(21)–OH(21)	0.99(3)	0.96(3)			
D(22)–OH(22)	0.95(3)	0.91(4)			
			Possible hydrogen bonds		
OH(1)···O(22)	3.01(1)	2.87(2)	D(1)···O(22)	2.15(2)	1.98(3)
OH(21)···O(21)	2.90(2)	2.95(2)	D(21)···O(21)	1.99(3)	2.10(4)
OH(22)···O(22)	2.95(2)		D(22)···O(22)	2.08(3)	
OH(1)–D(1)···O(22)	151(2)	151(3)			
OH(21)–D(21)···O(21)	154(2)	147(3)			
OH(22)–D(22)···O(22)	151(2)				

is less perturbed by the transformation. The slight modification of the structure mainly concerns the nitrate group position, especially the positions of the nitrogen and the two terminal oxygen atoms. This reorientation takes place in a plane almost parallel to (001), since the z coordinates of N and terminal O atoms are quite similar in the two phases. The angle between the directions O(21)–O(22) in the two phases is approximately 20°. Also, some changes in hydrogen bond strength are observed. First, O–D distances at room and high temperature are larger than the corresponding O–H distances evaluated by Effenberger, owing to the lack of precision on hydrogen atoms positions determined by X-ray diffraction. Second, the OH(1)···O(22) distance decreases from 3.01(2) to 2.87(2) Å between room and high temperature phases. Concerning D(22), no possible hydrogen bond occurs at high temperature.

It is interesting to note that this kind of small structural change is not unusual in copper compounds. Indeed, a similar effect has been observed for the related compound $Cu(OH)_2$ (19), in which a sudden shift of all reflections with $l \neq 0$, without significant changes in line intensities, occurs at about 60°C, which corresponds to an elongation of the c axis of 1% and a shortening of the b axis of 0.2%.

To conclude, this study has demonstrated again the power of sequential X-ray powder diffractometry for the study of the thermal behavior of solids. Indeed, it was possible to reveal the existence of small structural change in monoclinic copper hydroxide nitrate, when the connected energy effect, not detected in the previous studies, was masqueraded by the strong endothermic effect of the decomposition reaction occurring at a few degrees above the phase transition temperature. The reversible phase transition observed in monoclinic copper hydroxide nitrate is characterized by an elongation of about 0.3% of the linear unit cell parameters and a reduction of 2.4% of the angular parameter β. As shown by thermodiffractometry and precise DSC measurement, these changes between room temperature and 160°C do not result from a continuous deformation of the unit cell due to thermal expansion but from a phase transformation occurring at 158°C. The structural investigation from neutron powder diffraction data has shown that the main modification in the structure was a slight change in the orientation of the nitrate group just before the decomposition reaction.

ACKNOWLEDGMENTS

The authors are grateful to the Laboratoire Léon Brillouin for the provision of the research facilities, and to Mr. M. Pinot for his technical

support. They thank Prof. P.-E. Werner for helpful discussions, Dr. M. Matecki who carried out the DSC measurements, and Mr. G. Marsolier for his technical assistance in collecting X-ray powder diffraction data.

REFERENCES

1. P. Ramamurthy and E. A. Secco, *Can J. Chem.* **48,** 3510 (1970).
2. J. P. Auffrédic, D. Louër, and M. Louër, *J. Therm. Anal.* **16,** 329 (1979).
3. L. Ilcheva, M. Maneva, and P. Bozadziev, *J. Therm. Anal.* **16,** 205 (1979).
4. J. I. Langford and D. Louër, *J. Appl. Crystallogr.* **24,** 149 (1991).
5. W. Nowacki and R. Scheidegger, *Helv. Chim. Acta* **35,** 375 (1952).
6. H. Effenberger, *Z. Kristallogr.* **165,** 127 (1983).
7. M. Kempf and E.-J. Zehnder, *Z. Kristallogr.* **178,** 119 (1987).
8. B. Bovio and S. Locchi, *J. Crystallogr. Spectrosc. Res.* **12,** 507 (1982).
9. J. Plévert, J. P. Auffrédic, M. Louër, and D. Louër, *J. Mater. Sci.* **24,** 1913 (1989).
10. J. P. Auffrédic, J. Plévert, and D. Louër, *J. Solid State Chem.* **84,** 58 (1990).
11. D. Louër and J. I. Langford, *J. Appl. Crystallogr.* **21,** 430 (1988).
12. D. Louër and D. Weigel, *Bull. Soc. Fr. Mineral. Cristallogr.* **96,** 340 (1973).
13. A. Boultif and D. Louër, *J. Appl. Crystallogr.* **24,** 987 (1991).
14. A. D. Mighell, C. R. Hubbard, and J. K. Stalick," NBS*AIDS80: A FORTRAN Program for Crystallographic Data Evaluation." NBS (U.S.) Tech. note 1141.(NBS*AIDS83 is an expanded version of NBS*AIDS80) (1981).
15. J. Rodriguez-Carvajal, *in* "Collected Abstracts of Powder Diffraction Meeting," p. 127. Toulouse, France, 1990.
16. D. B. Wiles and R. A. Young, *J. Appl. Crystallogr.* **14,** 149 (1981).
17. "WYRIET Version 2, Powder Profile Refinement and Structure Analysis Package for Personal Computers." 1989.
18. R. K. Eby and F. C. Hawthorne, *Acta Crystallogr. Sect. B* **49,** 28 (1992).
19. U. W. Schönenberger, J. R. Günter, and H. R. Oswald, *J. Solid State Chem.* **3,** 190 (1971).